A Woman With Multiple Silicone Rupture Complicated by Inflammatory Breast Carcinoma

James Collins, MD

Keywords: radiology ■ MRI ■ chest ■ imaging ■ anatomy ■ inflammatory breast carcinoma ■ silicone rupture

J Natl Med Assoc. 2011;103:163-168

Author Affiliations: University of California at Los Angeles Medical School, Department of Radiological Sciences, Los Angeles, California.
Correspondence: James D. Collins, MD, University of California at Los Angeles, Department of Radiological Sciences, 10833 Le Conte Ave, BL-428 CHS/UCLA mail code 172115, Los Angeles, CA 90095 (jamesc@mednet.ucla.edu).

CLINICAL HISTORY

The patient in this case is a 51-year-old female with a history of breast reconstruction surgery going back to the age of 25 years, when she first had bilateral silicone breast implants constructed. The implants were associated with rapid development of severe capsular contraction, requiring both open and closed capsulotomy procedures. She had a total of 5 breast implants on the right and 6 on the left side. The last set of breast implants was removed 11 years ago. At that time, it was found that she had rupture of her left silicone implant with free silicone spill. She subsequently underwent surgery 9 years later for removal of free silicone from the left breast. She stated that after the procedure, her breasts were soft and normal in consistency. However, approximately 2 weeks before her scheduled brachial plexus examination, she presented with a left breast mass associated with transient skin erythema, which spontaneously resolved. Thereafter, she had a mammogram that displayed bilateral severely dense breasts with diffuse increased density of parenchyma on the left. Diffuse or inflammatory carcinoma was suspected.

The patient consulted and a fine-needle aspiration of the mass was performed 6 days later that displayed atypical cells. A core biopsy of the left breast mass followed, demonstrating ductal carcinoma with lymphatic invasion. The core pathology demonstrated 2 microscopic foci of invasive carcinoma measuring 0.03 cm each and separated by benign breast tissue. The 2 foci were morphologically different. One displayed tubular structures, but the other was poorly differentiated with lobular features.

It was unclear whether these 2 separate foci were portions of the same tumor with variation and morphologic pattern. Estrogen receptors were positive, progesterone receptors was positive, and her human epidermal growth factor receptor 2 was negative. Cancer antigen KI-67 was quite high at 28%.

PET scan of the body was positive only for a diffuse area in the left breast and axilla. Computed tomography (CT) scan of the chest, abdomen, and pelvis with contrast was positive for an infiltrating mass in the left breast with overlying skin thickening. There were borderline size left axillary lymph nodes associated with increased activity on positron emission tomography (PET) scan. There was also an 8-mm sclerotic foci in the posterior ileum on the right side, which was felt to be a bone island. A large mass in the lateral segment of the left liver lobe with dense nodular parenchyma enhancement appeared to be a hemangioma. This lesion was entirely negative on PET scan. A CT scan of the neck was negative.

The patient was classified as gravida 1, para 1, and aborta 0. She had menarche at age 13 and continued to have regular periods, with the last period occurring 1 week prior. She used birth control pills for 12 years and stopped 21 years ago. She had no fevers, sweats, chills, cough, wheezing, shortness of breath, abdominal pain, and/or abdominal distension, jaundice, bone pain or malaise.

PAST MEDICAL HISTORY

The patient tested positive for chickenpox, mumps, measles, and possible pertussis. She had a history of hypertension, which was under control. She had uterine myomectomy and breast implants as above given.

REVIEW OF SYSTEMS

Unremarkable except as above.

PHYSICAL EXAMINATION

Her blood pressure was 137/82 mm Hg; pulse, 63; respiration, 18 breaths/min; temperature, 97.9º. Her weight was 50.3 kg and height 5 ft 4 in. Palpable lymphadenopathy was present in the left axilla with a low left axillary node measuring 2.5 cm in diameter, and a high axillary node measuring 1.5 cm in diameter. She was also positive for a 9-cm hard mass affixed to the skin and

associated with peau d'orange changes in the skin. There were no skin or suspicious masses in the right breast.

Infiltrating ductal carcinoma changes, as above described, with positive estrogen and progesterone receptors indicated she should be considered T4B N1 MO (stage 3B).

Because she was concerned about the above findings, she wanted to rule out residual free silicone. She consulted with her physician who was aware of bilateral magnetic resonance imaging (MRI), magnetic resonance angiography (MRA), and magnetic resonance venography (MRV) of the brachial plexus to detect sites of brachial plexus compression and the detection of free silicone.

RADIOGRAPHIC AND MAGNETIC RESONANACE FINDINGS

The posteroanterior chest radiograph (Figure 1) displays drooping of the right shoulder as compared to the anterior rotated left; anterior rotated heads of the clavicles over the posterior fourth interscostal spaces; dense tissue within the left breast marginated by the lucency of the thickened skin as compared to the smaller right breast, and normal lungs and cardiomediastinal structures.

The lateral chest radiograph (Figure 2) displays mild rounding of the shoulders; narrowed anterior-posterior thorax, and the thin subcutaneous tissues; backward displaced manubrium placing the heads of the clavicles over the first ribs, the abnormal dense left breast obscuring the right breast.

CONCLUSION(S)

- Post silicone rupture left breast;
- Post bilateral silicone breast explantation;
- Mass left breast mass as above described;
- Bilateral round shoulders, droops right as compared to the anterior rotated left.

Multiplanar MRI cross-referenced the chest radiographs to display the resected left retro mammary space

Figure 1. Posterior-anterior view of the forward-drooping right shoulder as compared to the elevated left shoulder; anterior-rotated heads of the clavicles (C) over the asymmetric posterior fourth intercostal spaces (not labeled); bilateral asymmetric breast implants increasing the density of lungs, right greater than left; right hemidiaphragm (RD) slightly higher than the left (LD); bulging right axillary fold (axillary tail Spence) as compared to the left (not labeled. The lucent lateral margin (X) of the dense left breast reflects the thickening of the skin (peau d'orange).

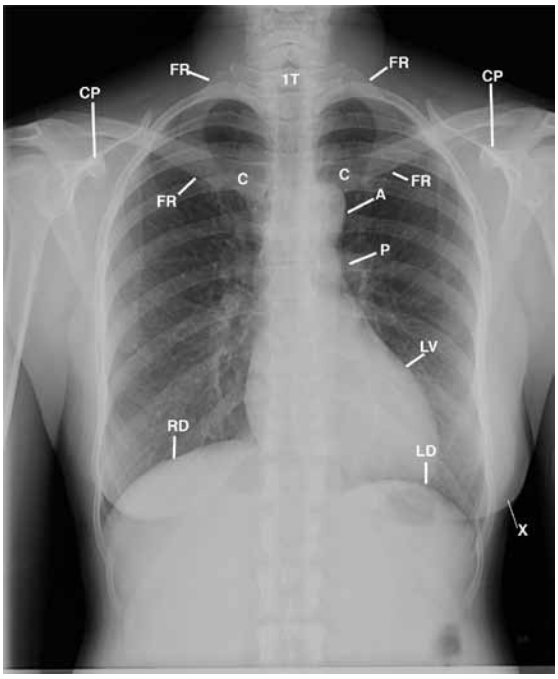

1T, first thoracic vertebra; A, aorta; CP, coracoid process; FR, first rib; LV, left ventricle; P, pulmonary artery.

Figure 2. Lateral chest view of the thorax that displays the dense breast implants (not labeled), kyphosis of the thoracic spine increasing the slope of the first ribs (FR) backwardly displacing the manubrium (M) placing the heads of the clavicles (not labeled) in close proximity to the first ribs, and rounding of the shoulders (X).

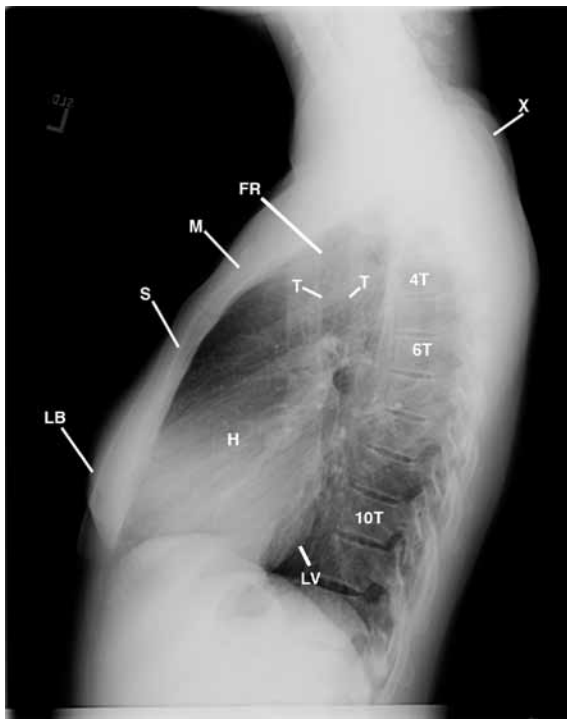

4T, 6T, 10T, thoracic vertebrae; H, heart; LB, left breast; LV, left ventricle; S, sternum; T, trachea.

(Figure 3) as compared to the right, abnormal gray proton dense lymphatics extending from the retro mammary space into the left breast mass, thick overlying skin left breast as compared to the right, mild costoclavicular compression of the subclavian veins evident by the mild decreased signal intensity of the subclavian veins crossed by the external jugular veins. Significant costoclavicular compression of the second division of the right subclavian artery was not displayed as compared to the second division of the left subclavian artery with binding nerve trunks.

Coronal, transverse, transverse oblique, and sagittal (Figure 4) sequences all cross-referenced the abnormal gray proton dense mass within the left breast with dilated gray proton-dense lymphatics extending from the chest wall into the thickened overlying skin.

The two-dimensional time-of-flight MRA/MRV (Figure 5) displayed diversion of venous return from the compressed left external jugular and subclavian veins evident by the dilated valveless left anterior jugular vein as compared to the valveless right anterior jugular vein.

The coronal fast spin echo (FSE) sequence (Figure 6) was acquired to display free silicone, silicone granulomas, and lymphatics within the chest wall and mass lesion as above described. Abnormal silicone was not displayed. High proton-dense right pleural fusion and irregular margins of the left breast with numerous lymphatics reflecting changes as above described.

Figure 3. Coronal magnetic resonance image of the thorax that displays scarring and metal clip over the right lateral chest wall; small lymph nodes (LN) marginating the left axillary vein (AXV); bilateral dilated gray proton dense subclavian veins (SV); dilated right external jugular vein (XJ); crimping of the right brachiocephalic artery (BR), and the small left internal jugular vein (J) as compared to the right internal jugular vein (J).

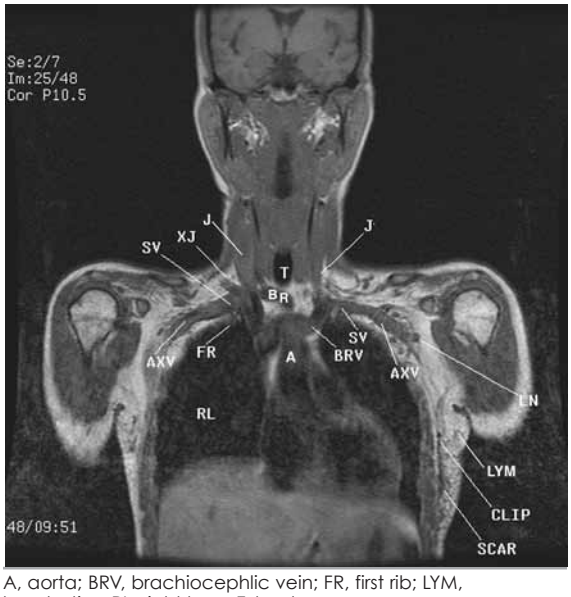

A, aorta; BRV, brachiocephlic vein; FR, first rib; LYM, lymphatics; RL, right lung; T, trachea.

CONCLUSION (S)

- Bilateral silicone breast explantation as per history;
- Post left silicone breast rupture as per history given;
- Inflammatory breast carcinoma with thickening of the skin (peau d'orange);
- Metastasis to left axillary and supraclavicular lymph nodes;
- Bilateral round shoulders, left greater than right;
- Scarring and fibrosis of the retro mammary spaces,

Figure 4. Left sagittal T1-weighted magnetic resonance image through the tumor (X) within the left breast. Observe the dilated high proton-dense veins (V) over the anterior and left lateral thorax (V).

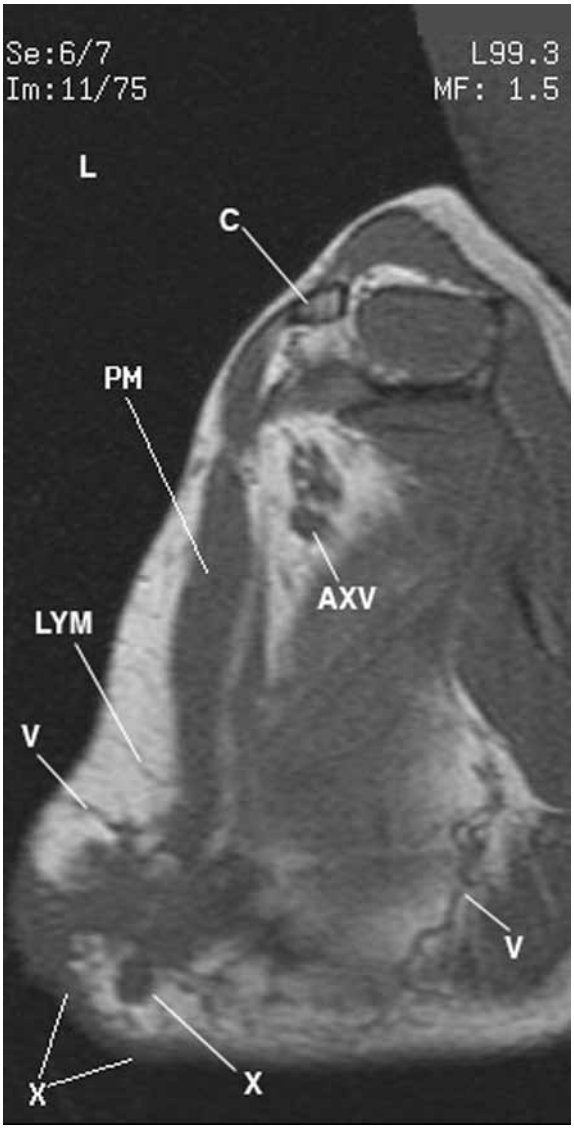

AXV, axillary vein; C, clavicle; L, left; LYM, lymphatic; PM, pectoralis major muscle.

left greater than right;
- Liver hemangioma as above;
- Small right pleural effusion;
- Bilateral abduction external rotation (AER) of the upper extremities triggered complaints left greater than right.

DISCUSSION

Inflammatory breast cancer is a rapidly growing advanced breast cancer that is usually not detected by mammograms or ultrasound. The cancer requires aggressive chemotherapy prior to surgery different from most types of breast cancer. Chemotherapy is begun within days of the diagnosis. Since the cancer grows in sheets and clumps of cells, lymphatics are often obstructed. Mammograms and ultrasound do not provide full field of view of the thorax to display the landmark anatomy of the adjacent lungs, arteries, veins, and lymphatics that may detect metastatic disease. CT and MRI examinations provide the radiologist an opportunity to superimpose knowledge of three-dimensional anatomy while interpreting plain radiographs. CT

Figure 5. Two-dimensional Time-of-Flight Magnetic Resonance Angiography/Magnetic Resonance Venography

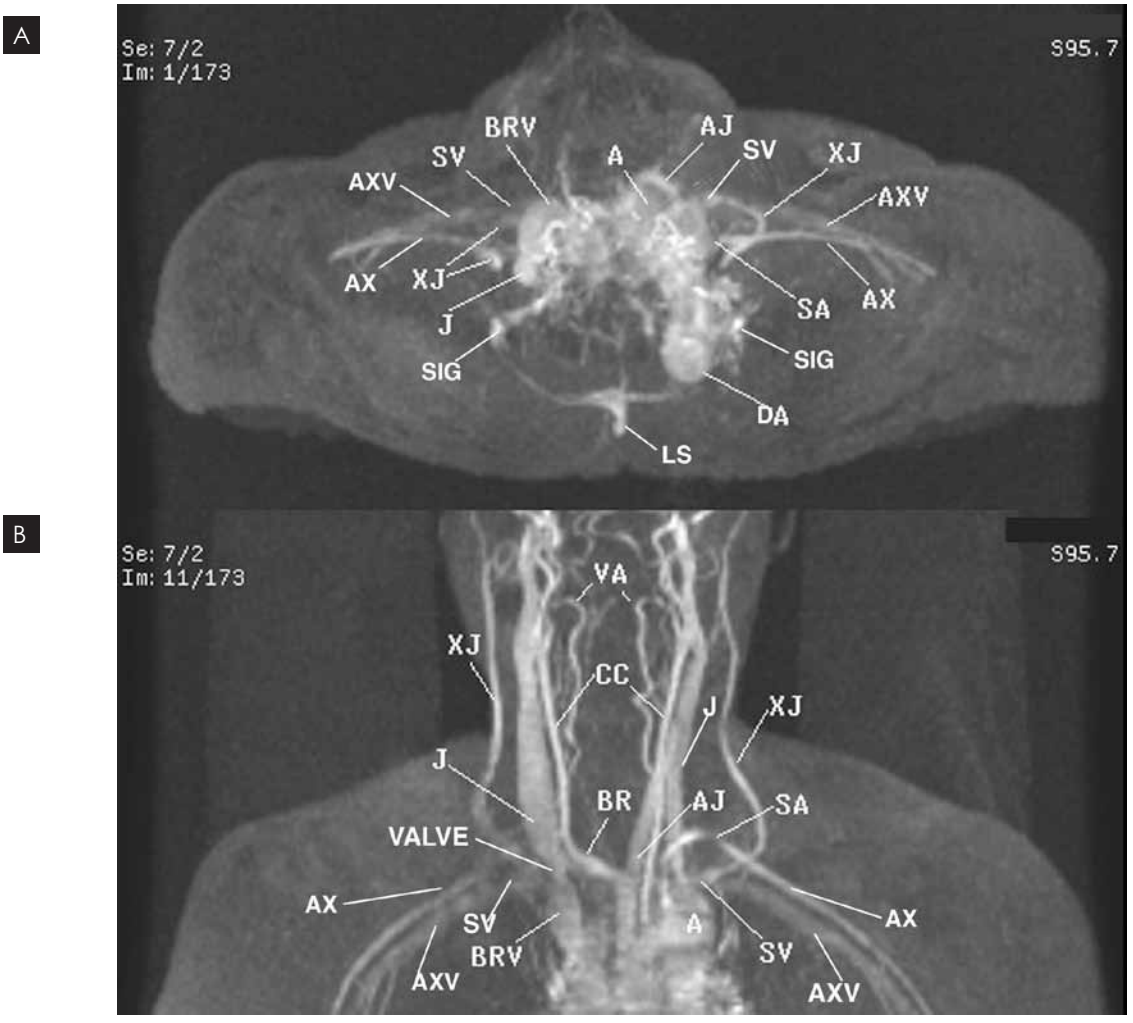

A, Stacked image displaying the decreased signal intensities of the compressed subclavian veins (SV) and the reciprocal dilated axillary veins (AXV); compressed decreased signal intensities of the second divisions of the subclavian arteries (SA) (site of the binding nerve trunks); dilated left valveless anterior jugular vein (AJ) reflecting diversion of venous return from the compressed left external jugular and subclavian veins greater than on the right.

B, Three-dimensional–reconstructed image that displays the decreased signal intensities of the compressed subclavian veins (SV) and the reciprocal dilated axillary veins (AXV); compressed decreased signal intensities of the second divisions of the subclavian arteries (SA) (site of the binding nerve trunks); dilated left valveless anterior jugular vein (AJ) reflecting diversion of venous return from the compressed left external jugular and subclavian veins greater than on the right.

A, aorta; AX, axillary artery; BR, brachiocephalic artery; CC, common carotid artery; DA, descending aorta; EX, external jugular vein; J, internal jugular vein; LS, longitudinal sinus; SIG, sigmoid sinus; Valve, inferior bicuspid valve of the right internal jugular vein).

extends the capabilities of x-ray imaging to obtain detailed transverse (axial) anatomic sections, but CT does not definitively separate tumors from vascular and/or neurovascular structures. CT-reconstructed imaging of soft-tissue anatomy is not satisfactory and detailed peripheral nerve imaging is not possible. MRI separates proton densities within organ systems and does not require reconstruction or repositioning of the patient. Multiplanar MRI displays the anatomy of the thorax, brachial plexus, and peripheral nerves for investigation by sequential imaging of landmark anatomy according to proton density distribution.[1]

Silicone breast implantations are used in surgical augmentation and reconstruction of the breast. Surgical breast implantation also contributes to scarring and fibrosis of the chest wall because the lymphatics are disrupted Following breast implantation, the silicone implants may harden, rupture into surrounding soft tissues and fascial planes involving the brachial plexus, as in our patient.[1] Complaints of severe bilateral breast pain, upper-extremity pain, tingling, and numbness (thoracic outlet syndrome); and chest wall lumps and bumps in the skin required that the breast implants be removed. Silicone breast implant ruptures demonstrate the pressure effects of mass-like lesions on subcutaneous tissues and on the brachial plexus. Following surgical removal of extravasated silicone and the ruptured capsule, lymphatic drainage is altered and may result in metaplasia and edema, which contribute to the pressure effects on the neurovascular bundles of the brachial plexus. Patients may present with low clavicles on the chest radiograph, which compounds the difficulty in distinguishing whether the complaint is due to fibrosis/scarring or costoclavicular compression by the low clavicle(s).[2] AER of the upper extremities in the sagittal MRI plane may be necessary to distinguish fibrosis and scarring from the compressive changes of the low clavicle(s). A tailored anatomic imaging approach to the

Figure 6. This is a coronal fast-spin echo (FSE) image displaying a superimposed grid at the same T1-weighted coronal sequence.

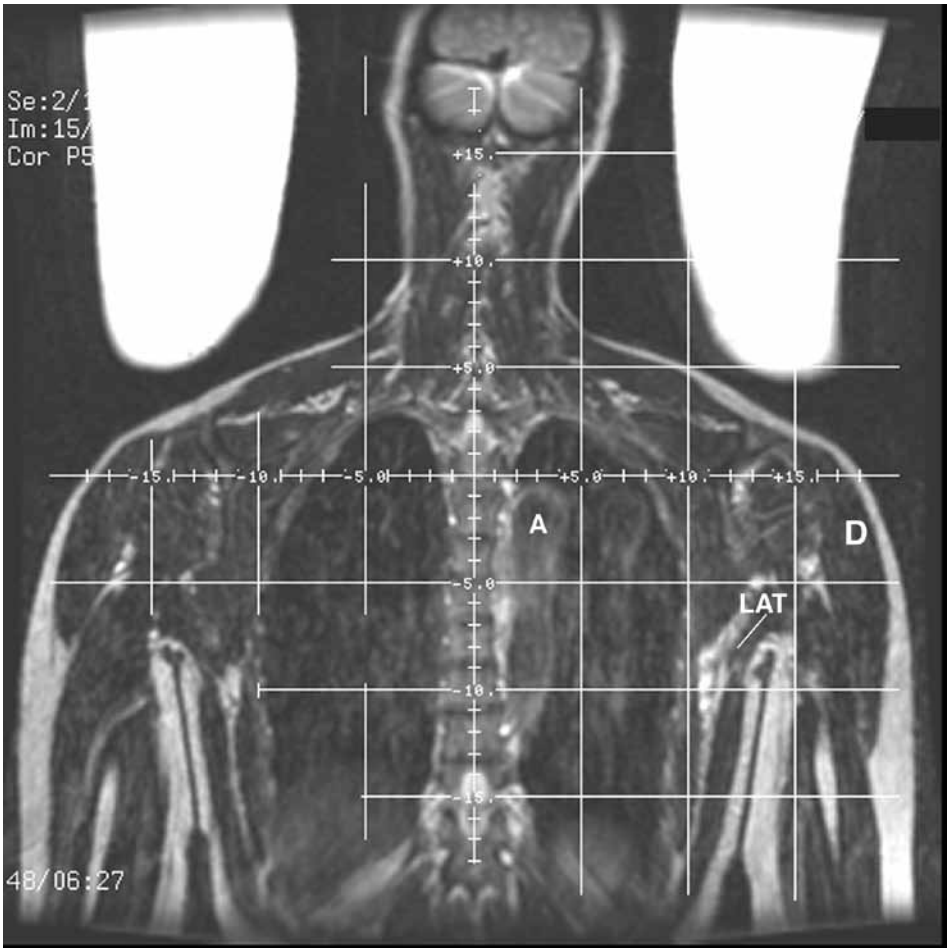

Observe the patient leaning left to limit the tension on the left painful shoulder and chest wall; dilated vascular structures medial to the left latissimus dorsi muscle (LAT), and the dilated small lymphatics within the subcutaneous tissues of the left upper extremity (limb, not labeled. D, deltoid muscle.

evaluation of the thorax using MRI allows distinguishing various pathological etiologies.[3]

Forty-two patients studied at the University of California–Los Angeles with the diagnosis of thoracic outlet syndrome had silicone breast implant ruptures that required surgical removal. At surgery, the breast implants were found to be encased in fibrous capsules. The surgeons opened the capsules to remove the harden ruptured breast implants and most of the extravasated silicone. Scar-like capsular tissue was also resected. After surgery, the patients continued to complain of "bumps in the skin," upper-extremity pain, tingling, and numbness, while raising their arms above shoulder height. They were referred for bilateral MRI of the brachial plexus to determine the site of brachial plexus neuropathy and the extent of chest wall and axillary fibrosis, and to detect the location of residual silicone deposits. MRI was performed on a 1.5-Tesla magnet (Signa; MR General Electric Medical Systems scanner, Milwaukee, Wisconsin) three-dimensional reconstruction MRI. T1-weighted and T2-weighted and/or FSE pulse sequences were performed in the coronal, transverse (axial), coronal oblique transverse, and sagittal planes using 4-mm slice thickness and 512 × 256 matrix size. Saline water bags were used to enhance the signal to noise ratio. Low signal intensities within the scalene triangles decreased anatomic detail of the cervical nerve trunks, obscured normal fascial plane between the pectoralis major and pectoralis minor muscles. At surgery, the low signal intensities proved to be fibrosis and silicone deposits; high proton densities on the chest wall proved to be deposits of silicone.[4]

The above patients wanted to link the silicone ruptures to collagen vascular diseases and other unrelated diseases. Of course, this was not the case. Certainly, they all had rounding of the shoulders and the clinical diagnosis of thoracic outlet syndrome with scarring and fibrosis causing costoclavicular compression of the bicuspid valves within the draining veins of the neck and supraclavicular fossae with lymphatics and compression of the subclavian and axillary arteries with binding nerve roots.

Our patient was made aware of the above chest radiographic and MRI findings. She wanted to relate the breast cancer to the silicone rupture, which could not be proven. She died 3 months later.

TAKE-HOME MESSAGE

Monitored bilateral MRI/MRA/MRV displays full field of view landmark anatomy by proton density that detects abnormalities beyond the appendages of the breast. Mammograms and ultrasound imaging do not provide full field of view to display landmark anatomy in silicone ruptures. Thoracic surgical resections may leave cells within severed lymphatics and thus allow recurrences at the site and/or distal to the surgical resection. Likewise, primary lesions in one lung may spread to the opposite lung by collateral lymph circulation, as suggested by the right pleural effusion in our patient. Obstructed lymphatics lose lymph fluid into the pleural space.[5] This patient is the only case of inflammation breast cancer that I am aware of related to multiple silicone implantation and explantation with silicone rupture, although not conclusively proven.

REFERENCES

1. Collins JD, Shaver M, Disher A, Miller TQ. Compromising abnormalities of the brachial plexus as displayed by magnetic resonance imaging. *Clin Anat*. 1995;l8:1-16.

2. Collins JD, Saxton E, Miller TQ, Ahn S, Gelabert H, Carnes A. Scheuermann's Disease As A Model Displaying the Mechanism of Venous Obstruction in Thoracic Outlet Syndrome and Migraine Patients: MRI and MRA. *J Natl Med Assoc*. 2003;4:298-306.

3. Collins JD, Shaver M, Batra P, Brown K, Disher A. Magnetic Resonance Imaging of Chest Wall Lesions. *J Natl Med Assoc*. 1991:4:352-360.

4. Collins JD, Miller TQ, Espinoza A. Silicone breast implant scarring: Brachial plexus neuropathy as display by MRI. *Federation Am Societies Exp Biol*. 1998;12:5:A1110.

5. Collins JD, Shaver M, Disher A, Batra P, Brown K, Miller TQ. Imaging the Thoracic Lymphatics: Experimental Studies of Swine. *Clin Anat*. 1991;4:433-446. ■